Colloid Polym Sci 274:269–278 (1996)

ORIGINAL CONTRIBUTION

K. Berger
K. Hiltrop

Characterization of structural transitions in the SLS/decanol/water system

Received: 18 November 1994
Accepted: 5 September 1995

Dr. K. Berger (✉) · K. Hiltrop
Physikalische Chemie
Universität Paderborn
33095 Paderborn, FRG

Abstract The ternary system sodium-dodecylsulphate (SLS)/decanol/water has been investigated at three different water contents and varying ratios of cosurfactant to surfactant by means of polarized optical microscopy, ^{2}H–NMR quadrupole splittings and small angle x-ray scattering. Upon addition of decanol a hexagonal phase transforms into a lamellar phase. For the highest water content of 0.65 no intermediate two-phase regions are detected but nematic phases are formed between. The lamellar phase at low cosurfactant content is very sensitive to changes of temperature and seems to be a so-called defective one with curved interfaces. From the scaling behavior it is concluded that the building units seem to be ribbons of increasing width on addition of cosurfactant or amphiphilic substance. By reaching a decanol mole fraction of 0.4 a "classical" lamellar phase with well-known behavior is formed. During these transformations the position of the first diffraction maximum changes gradually irrespective of phase transitions. The maximum mole fraction of cosurfactant the lamellar phase of our system can incorporate is 0.77.

Key words Lyotropic – liquid crystals – lamellar phase – SLS – x-ray diffraction

Introduction

In common amphiphile/water systems the one-dimensional lamellar phase (L_α) and the two-dimensional hexagonal phase (H) have a wide range of stability with respect to concentration and temperature [1, 2]. In the intermediate region between these "main" phases several phases with a relatively small range of stability like the nematic (N), rectangular (R) and cubic phase (V_1) have been detected [3–5].

The classification has mainly been performed by means of small-angle x-ray scattering (SAXS) experiments. The lattice of the liquid crystalline structures has been considered to be built up by rodlike aggregates of circular cross-section and infinite length in the case of the hexagonal phase and by bilayers of infinite lateral extension in the case of the lamellar phase [6].

Recent experiments have shown that the building blocks of the phases may differ from this "classical" picture. In the sodium decylsulphate/decanol/water system the addition of cosurfactant at constant water content leads to an increase of the lattice parameter that has been explained on the assumption of a noncircular cross-section of the aggregates [7]. At higher alcohol content a defective lamellar phase forms which shows diffuse scattering in oriented samples [8, 9] due to bilayers of finite lateral extension. The defects can be visualized as circular or elongated water pores piercing the lamellae [10]. A simple thermodynamic model which will be discussed in the third section can only qualitatively describe the variation of the

Colloid & Polymer Science, Vol. 274, No. 3 (1996)

defect volume with composition [11]. Defective lamellar phases have been observed in binary systems, too [12–15].

Studies of the cesium pentadecafluoro-octanoate/water system reveal that the transition from the discotic nematic to the defective lamellar phase is imperceptible from scattering experiments [16–18]. Even different nematic phases produce the same scattering pattern [19, 20]. Thus dramatic changes in the macroscopical appearance of lyotropic liquid crystalline phases need not be connected with strong changes of the microscopical building units. Some structural elements of preceeding phases can be found in succeeding phases and vice versa.

We have studied the transition from the curved interface of the hexagonal phase into the planar one of the classical lamellar phase in great detail. Our aim was to get further information about the phase stability in a common surfactant/cosurfactant/water system, the structural elements of these phases and the underlying principles that drive phase transitions. The work of Quist et al. [10] on the sodium dodecylsulphate/decanol/water system has been the starting point of our experiments.

The measurements have been performed by varying the amount of cosurfactant and surfactant, but leaving the overall volume fraction of the alkylchains constant. Thus our samples are located on three lines with different water content in the triangular phase diagram. With one line we touch the nematic phase (water content $c_W = 0.65$), the second line starts in the middle of the hexagonal phase ($c_W = 0.55$) whereas the third one begins at the boundary of the hexagonal phase ($c_W = 0.45$).

Experimental

Materials and sample preparation

SLS and decanol were of commercial origin (Merck, purity > 99%, for biochemical and surfactant investigations and Janssen, purity 99%), the H_2O was double destilled and millipore filtered.

The samples were prepared by weighing the appropriate amounts of SLS, decanol and water into glass tubes which were then sealed. They were vigorously mixed for several days in a Staudinger-wheel below 40 °C and then allowed to equilibrate at the desired temperature during at least 3 weeks. Just before performing the measurements the mass of the glass tubes was controlled and the composition was calculated assuming that the losses (< 1%) were caused by evaporation of water.

For the ^{2}H–NMR measurements the samples were prepared with a mixture of 90% H_2O and 10% D_2O in 5 mm NMR glass tubes which immediately were flame sealed. The samples were allowed to equilibrate during several weeks and the total mass was controlled, too.

Microscopy and NMR experiments

The samples were examined by polarized microscopy between glass plates in orthoscopic geometry. The characterization of the phases was done by comparison to standard textures [21]. Temperature control was achieved by a home-built stage which allowed regulation of temperature with an accuracy of better than 0.1 °C. Especially at the extreme phase boundaries, where even small changes in temperature cause phase transitions, the samples were additionally examined in sealed flat microslides (Camlab) [22].

For fluid samples two-phase regions could easily be detected by macroscopic phase separation after centrifugation. To ensure the phase boundaries ^{2}H–NMR measurements were performed using a Bruker WM 250 spectrometer working at a resonance frequency of 38.38 MHz. The temperature was controlled by airflow with an accuracy of ± 2 °C. The quadrupole splittings were obtained at the same temperature as the x-ray scattering experiments. To guarantee phase equilibrium the measurements were repeated after several weeks.

X-ray scattering

The main tool in our investigation was small-angle x-ray scattering. The experiments were performed at 25 °C for $c_W = 0.65$, at 30 °C for $c_W = 0.55$ and at 35 °C for $c_W = 0.45$.

The Bragg reflections were recorded in a Kratky-camera using monochromatic Cu–K_α radiation, $\lambda = 1.542 \cdot 10^{-10}$ m, with linear collimation. The scattering patterns were detected with a position-sensitive proportional counter equipped with a metallized quartz wire (Braun) to obtain a high resolution. Thus an uncertainty in $\vec{q}$ ($|\vec{q}| = 4\pi \sin\theta/\lambda$) of $\Delta|\vec{q}| = 2.5 \cdot 10^{-2}$ nm^{-1} was achieved. The uncertainty was approximately $0.5 \cdot 10^{-10}$ m for a lattice parameter of $35 \cdot 10^{-10}$ m and $2.5 \cdot 10^{-10}$ m for $80 \cdot 10^{-10}$ m. Since the orientation of the domains relative to the incident beam was unknown, no desmearing procedure was employed.

For each system at least two samples were prepared in Lindemann capillaries of 1 mm diameter which were flame sealed immediately after filling. The samples were investigated and then the tightness of the capillaries was tested in vacuum. A few days later the measurements were repeated. Thus every lattice parameter is the average value of at least four measurements.

To check orientation the two-dimensional scattering profiles were sometimes recorded on film in a Kiessig-camera, using pin-hole collimation and Ni filtered Cu–K_α radiation.

Results

Phase diagrams

The phase diagrams were mainly obtained by polarizing microscopy and ^{2}H–NMR-spectroscopy. Phase transitions in ionic surfactants are usually induced by changes in concentration and not by variations of temperature because the electrostatic interaction exceeds the thermal energy by far. Our results are presented as a function of the mole fraction of cosurfactant in the aggregate x_C which is calculated on the assumption that neither surfactant nor cosurfactant are water soluble.

Figures 1 and 2 show the phase sequences for water contents of $c_W = 0.65$ and $c_W = 0.55$. Due to hydrolysis of sodium dodecylsulphate at elevated temperatures the samples have only been examined up to 50 °C. For $c_W = 0.45$ no temperature induced transition was observed. The phase transitions at the corresponding temperatures are summarized in Table 1 and Fig. 3. A hexagonal phase (H) is formed at low content of cosurfactant. With decreasing amount of water the upper boundary is shifted to lower mole fractions of decanol. In the binary system the boundary of the hexagonal phase is nearly reached at $c_W = 0.45$. Hence slight amounts of decanol cause a phase transition.

The lamellar phase region (L_α) is entered at a nearly constant mole fraction of $x_C = 0.25$ independent of the water content. The width of the two-phase region hexagonal/lamellar increases with decreasing water content.

For $c_W = 0.65$ the transition into the lamellar phase is shifted to a significantly higher decanol content of $x_C = 0.30$. Nematic phases are formed in the intermediate region between the hexagonal and the lamellar phase. Within the limits of our measuring accuracy of $\Delta x_C \approx 0.02$ no two-phase region can be detected at this transition.

Figure 4 shows the ^{2}H–NMR-spectra for $c_W = 0.65$ and $x_C = 0.28$ immediately after transfer into the spectrometer and ten minutes later. The director aligns perpendicularly to the magnetic field; a homeotropic texture is observed in rectangular capillaries thus evidencing a discotic nematic phase (N_D) . At lower decanol content microscope observations revealed a homogeneous planar texture. Hence we assume this nematic phase to be a calamitic one (N_C) [22]. Up to now it is not clear if there is a biaxial nematic phase (N_B) between these two phases.

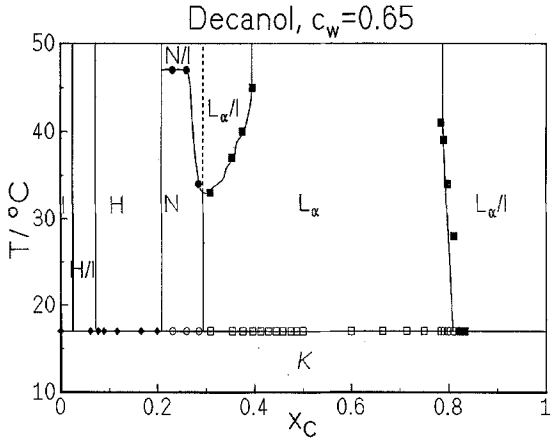

Fig. 1 Phase sequence for a water content of $c_W = 0.65$

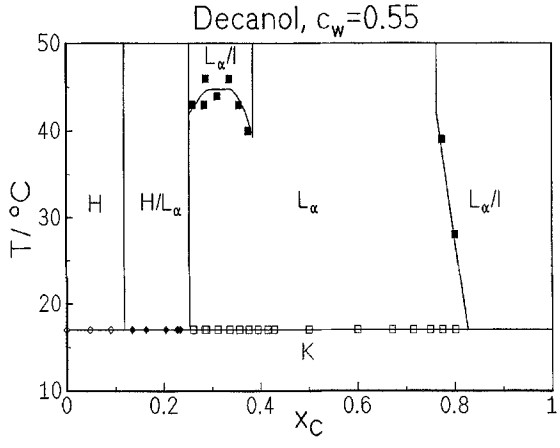

Fig. 2 Phase sequence for a water content of $c_W = 0.55$

Table 1 Phase transitions for the various water contents c_W as a function of the mole fraction of decanol in the hydrophobic part (± uncertainty of the last digit). I = isotropic phase, H = hexagonal phase, N_C = calamitic nematic phase, N_B = biaxial nematic phase, N_D = discotic nematic phase, L_α = lamellar phase

c_W	isothermal phase transitions $f(x_C)$								
0.65	I	$\xrightarrow{0.03(3)}$	H/I	$\xrightarrow{0.07(3)}$	H	$\xrightarrow{0.21(2)}$	N_C	$(\xrightarrow{0.25(2)}$	$N_B)$
		$\xrightarrow{0.27(1)}$	N_D	$\xrightarrow{0.30(2)}$	L_α	$\xrightarrow{0.82(1)}$	L_α/I		
0.55	H	$\xrightarrow{0.11(3)}$	$H/L_\alpha/I$	$\xrightarrow{0.25(2)}$	L_α	$\xrightarrow{0.77(2)}$	L_α/I		
0.45	H	$\xrightarrow{0.02(1)}$	H/L_α	$\xrightarrow{0.25(2)}$	L_α				

The ^{2}H–NMR Pake-spectrum for $c_W = 0.65$ and $x_C = 0.31$ in Fig. 5 shows that we have indeed a one-phasic uniaxial sample. At low cosurfactant content the lamellar structure transforms by slight changes of temperature into a two-phase region which is a strange behavior for ionic systems. The transition temperatures increase with rising

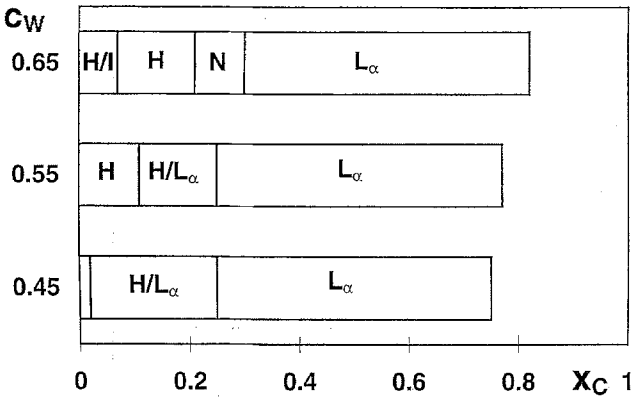

Fig. 3 Isothermal phase transitions for different water contents c_W

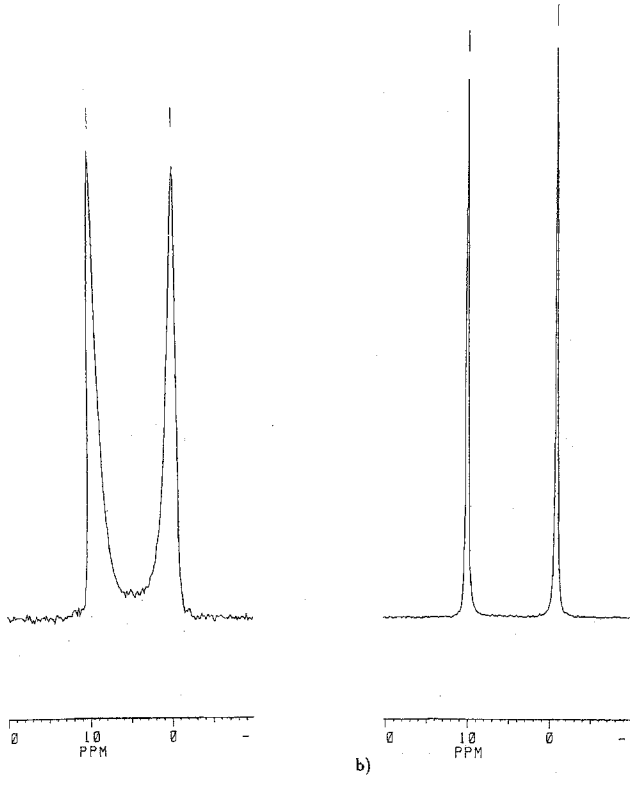

Fig. 4 ^{2}H–NMR spectrum for $c_W = 0.65$ and $x_C = 0.28$ a) immediately after transfer into the spectrometer b) ten minutes later

amount of alcohol and amphiphilic substance; hence for $c_W = 0.45$ no temperature induced phase transitions are observed.

At the phase boundary the lamellar and the discotic nematic phase have the same transition temperature of 33 °C. This is evidence for similar structural elements at the boundary of both phases. At $x_C > 0.40$ the lamellar phase becomes more stable with respect to variations of temperature.

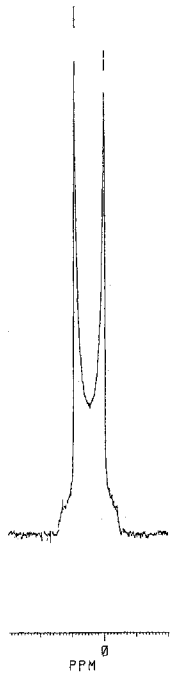

Fig. 5 ^{2}H–NMR spectrum for $c_W = 0.65$ and $x_C = 0.31$ after 10 min in the spectrometer

The transition from the lamellar phase into the two-phase region lamellar/isotropic occurs at a $x_C = 0.77$. The repulsive electrostatic force is apparently too weak to stabilize a lamellar phase furthermore.

Position of the first diffraction maxima

In Figs. 6–8 the positions of the first diffraction maxima, which are associated with the so-called interplanar distance d_0, are plotted versus x_C for the different water contents. In the case of the hexagonal phase the interplanar distance d_0 is connected to the lattice parameter d by $d = 2/\sqrt{3}\, d_0$.

In the hexagonal phase the interplanar distance d_0 remains nearly constant with varying cosurfactant concentration. In the other phases it changes continuously with the decanol content. Phase transitions as detected by polarized microscopy are not accompanied by a jump in the interplanar distance, only the slope of d_0 versus x_C changes.

In the lamellar phase two different regions can be distinguished.

– At low mole fractions of alcohol the lattice parameter depends strongly on the composition. This can be explained by varying amounts of water piercing the bilayer (see the third section).

– At medium concentrations of decanol the interplanar distance changes only slightly with x_C. Apparently the

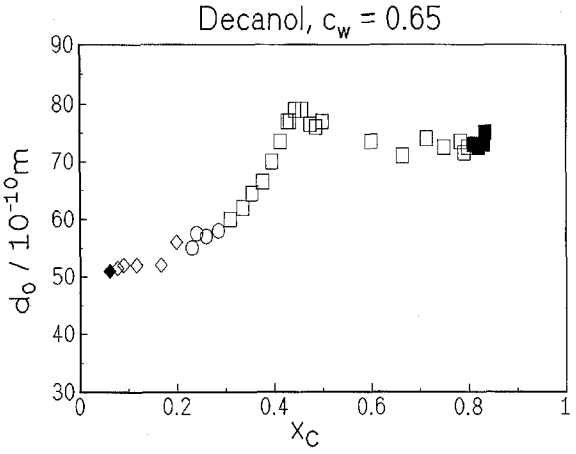

Fig. 6 Interplanar distance for a water content of $c_w = 0.65$. ◆ = multiphasic region, hexagonal parameter, ◇ = hexagonal region, ○ = nematic region, ■ = multiphasic region, lamellar parameter, □ = lamellar region

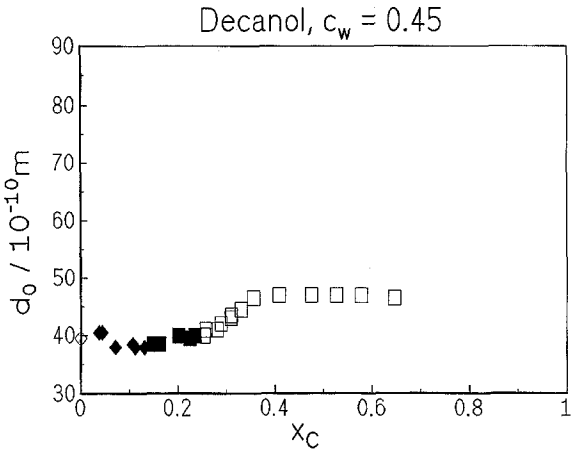

Fig. 8 Interplanar distance for a water content of $c_w = 0.45$. ◇ = hexagonal region, ◆ = multiphasic region, hexagonal parameter, ■ = multiphasic region, lamellar parameter, □ = lamellar region

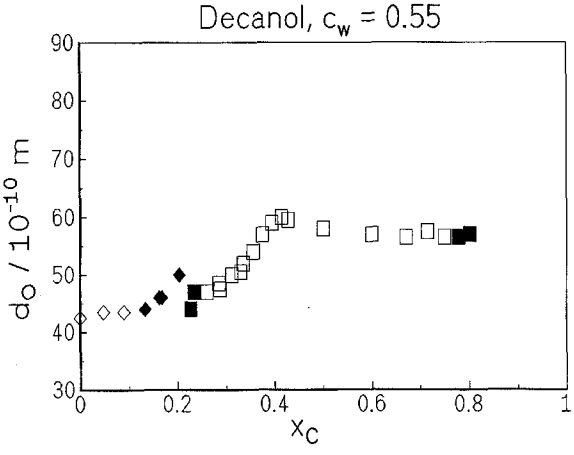

Fig. 7 Interplanar distance for a water content of $c_w = 0.55$. ◇ = hexagonal region, ◆ = multiphasic region, hexagonal parameter, ■ = multiphasic region, lamellar parameter, □ = lamellar region

lamellar structure consists of water-free bilayers of large lateral extension (see the third section).

The characteristic distances at the phase boundaries are given in Table 2. The data show that the smallest value of the lattice period in the lamellar structure d_0 at a transition across a two-phase region is closer to the value of d_0 than to the value of d in the neighboring hexagonal phase. Our experiments are in agreement with investigations of Hendrikx et al. in the related sodiumdecylsulphate (SdS)/decanol/water system [8]. From their x-ray data, we have calculated a constant interplanar distance of $37.5 \cdot 10^{-10}$ m in the hexagonal as well as in the neighboring lamellar phase and in the intermediate rectangular one.

Thus we can conclude that the two-dimensionally ordered aggregates of the hexagonal phase loose their positional order in one dimension on addition of cosurfactant. In the other direction the interplanar distances of both phases are equal at the phase transition. The one-dimensionally ordered lamellar structure forms on the lattice planes of the hexagonal phase. Their structural elements are strongly correlated to each other.

It is commonly found for calamitic nematic phases that there is only one broad diffraction maximum which is caused by short-range order of the micelles. Thus the average distance d_0 in the calamitic nematic phase should be comparable to the average distance of the aggregates in the hexagonal phase d. In contrast, our experiments reveal that the interplanar distances d_0 of 55 and $56 \cdot 10^{-10}$ m in the two phases are comparable. Furthermore, the value of d_0 remains constant through the transition from a discotic

Table 2 Characteristic distances at the extreme phase boundaries for the various water contents c_w

c_w	Hexagonal phase		Nematic phase		Lamellar phase
	$d_0/10^{-10}$ m	$d/10^{-10}$ m	$d_0(N_C)/10^{-10}$ m	$d_0(N_D)/10^{-10}$ m	$d_0 = d/10^{-10}$ m
0.65	56.0	64.7	55.0	58.0	60.0
0.55	43.5	50.2	–	–	47.0
0.45	39.5	45.6	–	–	40.0

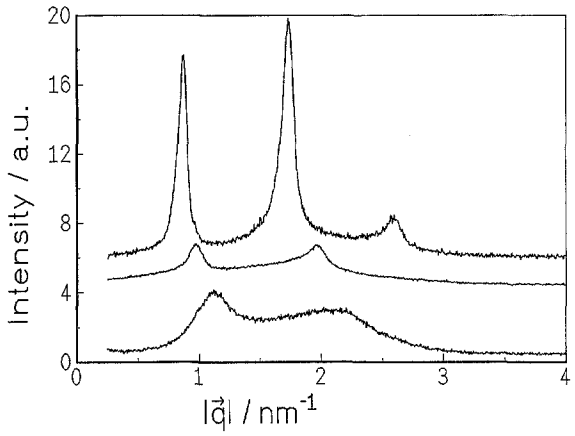

Fig. 9 One-dimensional scattering profiles for a water content of $c_W = 0.65$. top = mole fraction of decanol $x_C = 0.503$, middle = mole fraction of decanol $x_C = 0.354$, bottom = mole fraction of decanol $x_C = 0.260$

nematic to a lamellar phase. This may again point to similar structural elements at the phase boundaries.

The evolution of the one-dimensional diffraction pattern from the nematic phase into the classical lamellar structure can be seen in Fig. 9.

In the nematic phase two diffraction maxima with large widths are detected. The occurrence of a second-order reflection indicates that there is not only an orientational order like in ordinary nematic phases, but a pseudo-lamellar arrangement of the aggregates as well. By addition of alcohol a lamellar phase forms continuously, the diffraction maxima sharpen and are shifted towards lower values of $|\vec{q}|$. At higher cosurfactant content even a third-order reflection is detectable.

A calculation of the order parameter or the electron density profile of a single lamella has not been performed because of the unknown orientation of the domains with respect to the incident x-ray beam.

Another explanation for the strange scattering profiles is that in the narrow regime of the nematic phase not a structure element of the phase itself is detected but the fluctuations of neighboring phases. These fluctuations are caused by clusters with long-range order and grow in intensity by reaching the boundary of the nematic phase. This assumption can explain the position and the intensity of the diffraction maxima at the phase transition as well.

Bilayer thickness

The hexagonal phase

The diameter of the hydrophobic part of the surfactant aggregates d_u can be calculated from the x-ray data and the volume fraction of the hydrocarbon chains ϕ_u using the group volumes in [23].

According to [6] the diameter of the cylindrical aggregates as a function of the interplanar distance d_0 is:

$$d_u = d_0 \left(\frac{8}{\sqrt{3}\pi}\right)^{1/2} \phi_u^{1/2} . \quad (1)$$

From Figs. 6–8 we can conclude that the interplanar distance at a fixed water content in the hexagonal phase and consequently d_u remain constant. Only in the two-phase region does the hexagonal interplanar distance seems to increase slightly. However in that case the lattice parameter could not be determined with high accuracy because of macroscopic phase separation.

Table 3 indicates that the diameter of the cylinders does not vary with dilution. The interplanar distance scales with $\phi_u^{1/2}$ showing that water is incorporated into two dimensions (see later). This is a good evidence of a classical hexagonal phase of long cylindrical micelles.

The calculated diameter of $\approx 32 \cdot 10^{-10}$ m (see Table 3) is only slightly smaller than the length of two dodecylchains in all-trans-conformation of $33.4 \cdot 10^{-10}$ m. But in lyotropic liquid crystalline phases the alkylchains are in a "melted" and not in a "crystalline" state. Hence we would expect the diameter to be much smaller than the all-trans value. The observed large diameter suggests that the cross-section of the aggregates in the hexagonal phase is already noncircular but appears to be circular on average [24].

The classical lamellar phase

Figures 10, 11 and 12 show the dependence of the apparent bilayer thickness d_u, which is the product of ϕ_u and the lattice parameter d_0 of the lamellar phase, on the decanol content.

A bilayer of pure surfactant exists for $x_C = 0$; its thickness is limited by twice the length of a dodecylchain in all-trans conformation. The maximal thickness of a pure cosurfactant lamella is given by the length of two decanol molecules. Hence we expect a linear relation between the

Table 3 Parameters of the hexagonal phase c_W = water content, ϕ_u = volume fraction of the alkylchains, x_C = mole fraction of decanol, d_0 = interplanar distance of the hexagonal phase, d_u = cylinder diameter in the hexagonal phase

c_W	ϕ_u	x_C	$d_0/10^{-10}$ m	$d_u/10^{-10}$ m
0.65	0.279	0.09	52.0	33.3
0.55	0.364	0.09	43.5	31.8
0.45	0.442	0	39.5	31.8

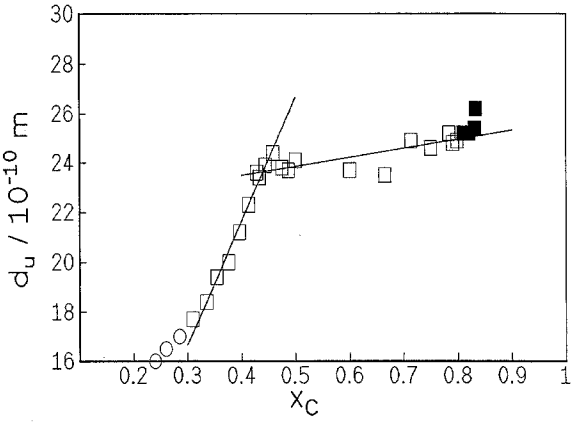

Fig. 10 Apparent bilayer thickness for a water content of $c_W = 0.65$. ○ = nematic region, □ = lamellar region, ■ = multiphasic region, lamellar parameter

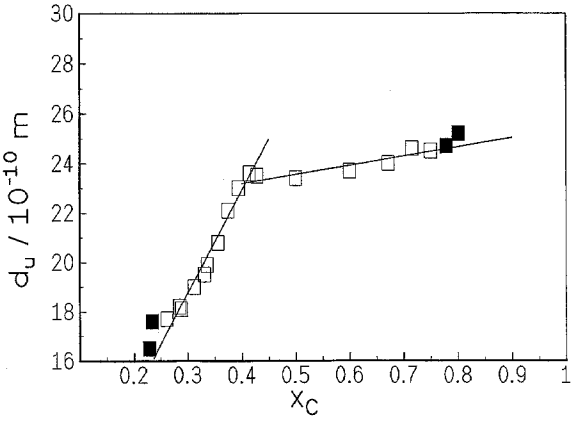

Fig. 11 Apparent bilayer thickness for a water content of $c_W = 0.55$. ■ = multiphasic region, lamellar parameter, □ = lamellar region

bilayer thickness of a classical lamellar phase $d_{c,u}$ and x_C or $d_{c,u} = a + b\,x_C$. The limiting values of the coefficients are $a = 33.4 \cdot 10^{-10}$ m and $b = -5.1 \cdot 10^{-10}$ m.

The fits of the experimental results for medium fractions of cosurfactant where the lattice parameter is nearly independent of composition are given in Table 4. The correlation coefficients of $r > 0.75$ show that the linear dependence is a reasonable approximation.

The y-interception of $21 \cdot 10^{-10}$ m is independent of the water content and amounts to about 65% of the fully extended length of two chains. The hydrophobic tail is shortened by gauche-conformations demonstrating its high flexibility. The observed ratio is in good agreement with results in other amphiphilic systems with bilayer thicknesses of 60–90% of the limiting values [1, 4].

Surprisingly, the bilayer thickness is not decreasing with the decanol content but increasing with a slope b of about $4 \cdot 10^{-10}$ m. One explanation is that the distance

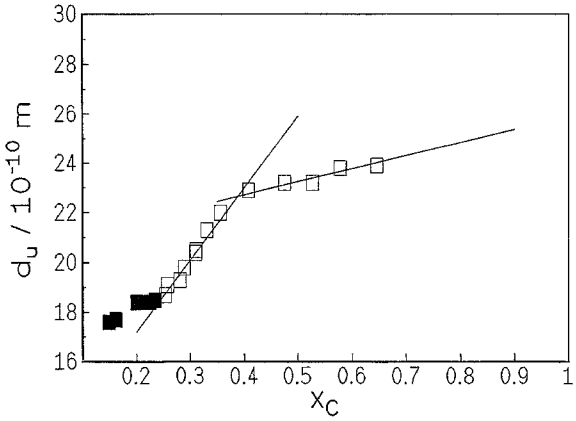

Fig. 12 Apparent bilayer thickness for a water content of $c_W = 0.45$. ■ = multiphasic region, lamellar parameter, □ = lamellar region

Table 4 Parameters of the classical lamellar phase ($d_{c,u} = a + bx_C$) c_W = water content a = bilayer thickness for $c_W = 0$, b = slope of the bilayer thickness, r = correlation coefficient

c_W	$a/10^{-10}$ m	$b/10^{-10}$ m	r
0.65	22.0	3.7	0.75
0.55	21.7	3.7	0.90
0.45	20.6	5.3	0.90

between neighboring headgroups is reduced on addition of cosurfactant due to the weakened electrostatic repulsion. The area per amphiphilic molecule decreases and because of the constant hydrophobic volume the aliphatic chain is elongated. The reduced flexibility of the hydrocarbon chains has already been detected in other ternary surfactant systems [25].

A further explanation is that the ionic sulphate group is strongly hydrated so that the neighboring methylene groups are pulled out of the unpolar bilayer into the water region. Thus the effective hydrophobic length of the surfactant is reduced and is exceeded by the length of the cosurfactant.

The non-classical lamellar phase

At low mole fractions of cosurfactant the apparent bilayer thickness depends strongly on its composition. Obviously, this behavior is correlated to the formation of curved interfaces near the hexagonal phase. By approaching the phase boundary increasing amounts of water enter the bilayer as defects. Quist et al. [10] have already shown that real bilayer thinning by interdigitating alkylchains cannot explain these observations.

Table 5 Parameters of the non-classical lamellar phase ($d_u = a + bx_C$) c_W = water content, a = apparent bilayer thickness for $c_W = 0$, b = slope to the apparent bilayer thickness, r = correlation coefficient, x_i = mole fraction of decanol in the point of intersection, $d_{u,i}$ = bilayer thickness in the point of intersection, $\psi_w^{max} W$ = maximum volume fraction of water in the lamella

c_W	$a/10^{-10}$ m	$b/10^{-10}$ m	r	x_i	$d_{u,i}/10^{-10}$ m	ψ_W^{max}
0.65	1.7	49.9	0.99	0.44	23.6	0.23
0.55	6.3	41.5	0.99	0.41	23.2	0.22
0.45	11.4	29.0	0.99	0.39	22.7	0.15

In a first approximation we have assumed that the bilayer thickness depends linearly on the cosurfactant content as in the case of medium decanol content. The fits gave the results summarized in Table 5. As shown in Figs. 10–12 the assumption is correct. Only at very low alcohol concentrations is the apparent bilayer thickness slightly increased.

The calculated values of a for these low decanol contents are small and cannot be regarded as the real bilayer thickness in the binary system. The y-interception a decreases while the slope b increases with the water content c_W. Thus the defect volume increases with c_W at a fixed bilayer composition x_C.

In a thermodynamic model [26] two contrary effects are considered to participate in defect formation. The model starts with a classical lamellar phase of alternating water and surfactant sheets. In a first step of the gedanken experiment water is taken away from the interbilayer space, therefore reducing the aqueous layer thickness. Due to the enhanced electrostatic repulsion of the charged bilayers the energy of the system rises. Hence the smaller the initial distance between the charged sheets the more energy is necessary to reduce the separation for a certain distance. In a second step the surplus water is placed as defects in the bilayer, leaving the aqueous layer thickness constant. The formation of curved interfaces increases the distance between neighboring charged head-groups and thus causes a negative free energy change. According to the model, defect formation should be favored by high water contents. Thus the lattice parameter of the non-classical lamellar phase should increase stronger with the cosurfactant content for high dilutions.

Although the model gives a qualitatively correct description for the experimental observations it cannot quantitatively account for our data. Especially the variation of the defect volume with the chemical composition has not been considered by the model.

On the assumption that the real bilayer thickness in this region obeys the linear dependence of the classical lamella (see Table 4), we have determined the maximum

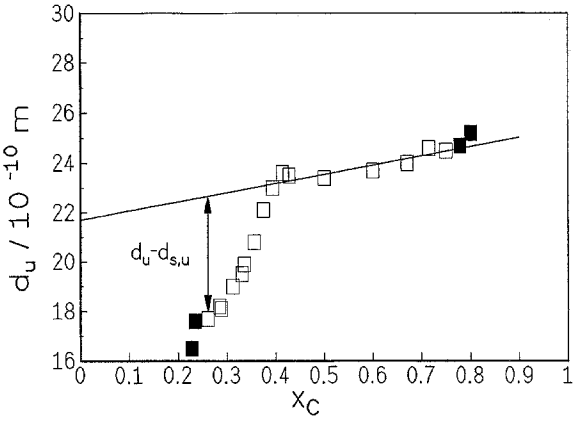

Fig. 13 Determination of the maximum volume fraction of water ψ_W^{max} the bilayer of a lamellar phase can incorporate

volume fraction of water (ψ_W^{max}) the lamellar phase can incorporate. As shown in Fig. 13 it has been calculated by comparison of the bilayer thickness for the classical lamellar ($d_{c,u}$) phase with the apparent bilayer thickness of the non-classical lamellar phase (d_u) for the lowest mole fraction of decanol where the L_α-phase is stable.

$$d_u = d_{c,u}(1 - \psi_W) \,. \tag{2}$$

According to Table 5 the bilayer of a lamellar phase can incorporate larger amounts of water at high dilution. At $c_W = 0.65$ the defect volume is not increasing any more because an intermediate nematic phase is formed. If the nematic phase were regarded as a one-dimensional ordered structure (see the x-ray results), the maximum water uptake would be $\psi_W^{max} = 0.28$.

The point of intersection of the linear fits at high and low decanol content indicates the transition of a defective into a defect-free classical bilayer. As seen from Table 5 these points have the coordinates $x_i = 0.4$ and $d_{u,i} = 23 \cdot 10^{-10}$ m irrespective of the water content.

Since the classical lamellar phase forms at a constant mole fraction of cosurfactant the value of a which is the point of intersection with the d-axis decreases with increasing slope b.

This intermediate one-dimensional ordered phase is called a defective lamellar phase and denoted by L_α^H.

Scaling behavior

Because no diffuse scattering in oriented samples could be detected with our experimental equipment, nothing can be said about the defect topology.

In our case a successful approach to get further information about the building units is to compute the

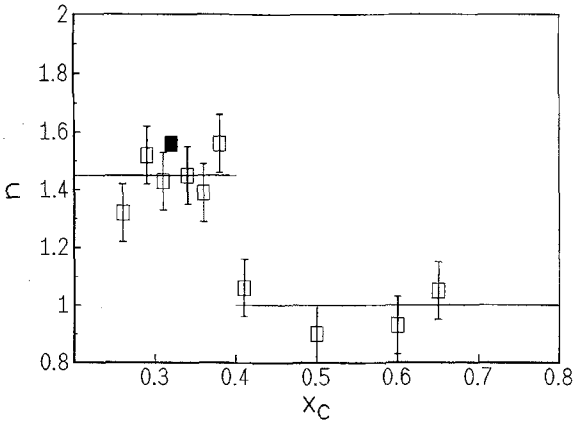

Fig. 14 Scaling exponent of the nematic and lamellar phase. □ = own measurements, ■ = measurements of Quist et al. [10]

variation of the dimensions with the water content [18]. If the size of the aggregates remains constant upon dilution then the characteristic dimensions of the system will scale with $d \propto \phi^{-1/n}$, where n denotes the dimensionality of the system. For an ideal micellar phase $n = 3$, for a hexagonal phase the dimensionality is $n = 2$ and a lamellar phase composed of bilayers of infinite lateral extension is an example for $n = 1$. We have already shown that the hexagonal phase in the SLS/decanol/water system has a two-dimensional scaling behavior.

So we have calculated the dimensionality n for varying compositions of the bilayer by fitting the original data of the nematic and the lamellar phase to:

$$\ln d_0 = a - \frac{1}{n} \ln \phi_a$$

Additionally, we have treated the x-ray data of Quist et al. [10] in the same way to compare their measurements with ours. The scaling behavior as a function of the mole fraction of decanol in the hydrophobic part is plotted in Fig. 14.

Above $x_C > 0.4$ the one-dimensional scaling of a classical lamellar phase is observed. From the fluctuations of the dimensionality we can deduce an accuracy of $\Delta n = \pm 0.1$.

Up to $x_C = 0.4$ the structure scales with $n = 1.45$. This looks like an average of one- and two-dimensional growth. The structural building units can be described as ribbon-shaped bilayers, with growing width upon increasing amphiphile concentration. The detected scaling behavior clearly differs from the true two-dimensional one obtained for the defective structure in the cesium pentadeca-fluoro-octanoate/water system [18].

At $x_C > 0.4$ there seems to be a sharp transition into the one-dimensional scaling of a classical lamellar phase. We conclude that the defect water is expelled from the bilayer until a classical bilayer is formed. The transformation $L_\alpha^H \rightarrow L_\alpha$ can be described as a first order transition.

The nematic phase show the same scaling behavior as the defective lamellar phase. Both phases seem to consist of similar structural elements.

Conclusions

We have shown that the interplanar distance changes gradually from the hexagonal into the lamellar phase without any discontinuity until the lattice parameter reaches its limiting value at a mole fraction of decanol of 0.4. At this transition the aggregates of the hexagonal phase seem to loose their two-dimensional correlation first so that a lamellar structure is formed. This demonstrates that the structural elements of neighboring phases are strongly related and may differ from the classical picture at these boundaries. The defective lamellar phase scales with a dimensionality of 1.45, between a one- and two-dimensional structure. Hence the microscopical building units can be described as ribbons of increasing width.

Independent of the water content the defective lamellar phase transforms at $x_C = 0.4$ sharply into a classical bilayer phase with well-known behavior. The transition is characterized by a continuous change of the layer period d_0 but a jump in the slope of d_0 versus x_C.

The so-called nematic phase shows two diffraction maxima and identical scaling as the defective lamellar phase. The similar physical properties of these phases will be discussed in a separate article.

Acknowledgement We would particularly like to thank Prof. M. Holmes for helpful discussions and G. Jünnemann for technical assistance.

References

1. Ekwall P (1975) Composition, properties and structures of . . . In: Brown GH (ed) Advances in Liquid Crystals New York, Academic Press, p 1
2. Luzzati V (1968) X-ray Diffraction Studies of Lipid Water Systems In: Chapman D (ed) Biological Membranes. Academic Press, New York, p 71
3. Charvolin J (1989) Lyotropic Liquid Crystals, Structures and Phase Transitions In: Risto T, Sherrington D (eds) Phase Transitions in Soft Condensed Matter. NATO ASI Ser B New York, Plenum Press p 95

4. Tiddy GJT (1980) Physics Report 57:1
5. Hiltrop K (1994) Lyotropic Liquid Crystals In: Stegemeyer H (ed) Liquid Crystals. Steinkopff, Darmstadt, p 143
6. Husson F, Mustacchi H, Luzzati V (1960) Acta Cryst 660
7. Hendrikx Y, Charvolin J (1988) Liq Cryst 3:205
8. Hendrikx Y, Charvolin J (1992) Liq Cryst 11:677
9. Hendrikx Y, Charvolin J, Kekicheff P, Roth M (1987) Liq Cryst 2:677
10. Quist PO, Halle B (1993) Phys Rev E 47: 3374
11. Quist PO, Fontell K, Halle B (1994) Liq Cryst 16:235
12. Funari SS, Holmes MC, Tiddy GJT (1994) J Phys Chem 98:3015
13. Funari SS, Holmes MC, Tiddy GJT (1992) J Phys Chem 96:11029
14. Leaver MS, Holmes MC (1993) J Phys II France 3:105
15. Kekicheff P, Cabane B, Rawiso M (1984) J Phys Lett Paris 45:813
16. Boden N, Corne SA, Homes MC, Jackson PH, Parker D, Jolley KW (1986) J Phys France 47:2135
17. Boden N, Corne SA, Jolley KW (1987) J Phys Chem 91:4092
18. Holmes MC, Leaver MS, Smith AM (1995) Langmuir 11:356
19. Galerne Y, Figueiredo Neto AM, Liébert L (1987) J Chem Phys 87:1851
20. Figueiredo Neto AM, Galerne Y, Liébert L (1991) Liq Cryst 10:751
21. Rosevear FB (1954) J Am Oil Chem Soc 31:629
22. Holmes MC, Boden N, Radley K (1983) Mol Cryst Liq Cryst 100:93
23. Tanford C (1980) The Hydrophobic effect. 2nd ed. New York, Wiley, p 52
24. Hagslätt H, Söderman O, Jönsson B (1994) Liq Cryst 17:157
25. Klason T, Henriksson U (1982) The Motional State of Hydrocarbon Chains in the Ternary System ... In: Mittal KL, Fendler EJ (eds) Solution Behaviour of Surfactants. Plenum, New York, p 417
26. Bagdassarian CK, Roux D, Ben-Shaul A, Gelbart WM (1991) Chem Phys 94: 3030